

# Improving Ensemble Robustness by Collaboratively Promoting and Demoting Adversarial Robustness

Anh Bui<sup>1</sup>, Trung Le<sup>1</sup>, He Zhao<sup>1</sup>  
Paul Montague<sup>2</sup>, Olivier deVel<sup>2</sup>, Tamas Abraham<sup>2</sup>, Dinh Phung<sup>1</sup>

<sup>1</sup>Monash University

<sup>2</sup>Defence Science and Technology Group, Australia  
tuananh.bui@monash.edu

## Abstract

Ensemble-based adversarial training is a principled approach to achieve robustness against adversarial attacks. An important technique of this approach is to control the transferability of adversarial examples among ensemble members. We propose in this work a simple yet effective strategy to collaborate among committee models of an ensemble model. This is achieved via the secure and insecure sets defined for each model member on a given sample, hence help us to quantify and regularize the transferability. Consequently, our proposed framework provides the flexibility to reduce the adversarial transferability as well as to promote the diversity of ensemble members, which are two crucial factors for better robustness in our ensemble approach. We conduct extensive and comprehensive experiments to demonstrate that our proposed method outperforms the state-of-the-art ensemble baselines, at the same time can detect a wide range of adversarial examples with a nearly perfect accuracy.<sup>1</sup>

## Introduction

Deep neural networks have experienced great success in many disciplines (I. Goodfellow, Y. Bengio, and Courville, 2016), such as computer vision (K. He et al., 2016), natural language processing and speech processing (Vaswani et al., 2017). However, even the state-of-the-art models are reported to be vulnerable to adversarial attacks (Biggio et al., 2013; I. J. Goodfellow, Shlens, and Szegedy, 2015; Szegedy et al., 2014; N. Carlini and D. Wagner, 2017; Madry et al., 2018; Athalye, Nicholas Carlini, and David Wagner, 2018), which is of significant concern given the large number of applications of deep learning in real-world scenarios. It is thus urgent to develop deep learning models that are robust against different types of adversarial attacks. To this end, several adversarial defense methods have been developed but typically addressing the robustness within a single model (e.g., Papernot, P. D. McDaniel, et al., 2016; Moosavi-Dezfooli, Fawzi, and Frossard, 2016; Madry et al., 2018; Qin et al., 2019; Shafahi et al., 2019). To cater for more diverse types of attacks, recent work, notably (W. He et

al., 2017; Tramèr, Kurakin, et al., 2018; Strauss et al., 2017; X. Liu et al., 2018; Pang, Xu, et al., 2019), has shown that ensemble learning can strengthen robustness significantly.

Despite initial success, key principles for ensemble-based adversarial training (EAT) largely remain open. One crucial challenge is to achieve minimum ‘transferability’ between committee members to increase robustness for the overall ensemble model (Papernot, P. McDaniel, and I. Goodfellow, 2016; Yanpei Liu et al., 2016; Tramèr, Kurakin, et al., 2018; Pang, Xu, et al., 2019; Kariyappa and Qureshi, 2019). In (Kariyappa and Qureshi, 2019), robustness was achieved by aligning the gradient of committee members to be diametrically opposed, hence reducing the shared adversarial spaces (Tramèr, Papernot, et al., 2017), or the transferability. However, the method in (Kariyappa and Qureshi, 2019) was designed for black-box attacks, thus still vulnerable to white-box attacks. Furthermore, attempting to achieve gradient alignment is unreliable for high-dimensional datasets and it is difficult to extend for ensemble with more than two committee members. More recently (Pang, Xu, et al., 2019) proposed to promote the diversity of non-maximal predictions of the committee members (i.e., the diversity among softmax probabilities except the highest ones) to reduce the adversarial transferability among them. Nonetheless, the central concept of transferability has not been systematically addressed.

Our proposed work here will first make the concept of adversarial transferability concrete via the definitions of secure and insecure sets. To reduce the adversarial transferability and increase the model diversity, we aim to make the insecure sets of the committee models as disjoint as possible (i.e., lessening the overlapping of those regions) and challenge those committee members with divergent sets of adversarial examples. In addition, we observe that lessening the adversarial transferability alone is not sufficient to ensure accurate predictions of the ensemble model because the committee member that offers inaccurate predictions might dominate the final decisions. With this in mind, we propose to realize what we call a “transferring flow” by collaborating robustness promoting and demoting operations. Our key principle to coordinate the promoting and demoting operations is to promote the prediction of one model on a given adversarial example and to demote the prediction of another model on this example so as to maximally lessen the neg-

Copyright © 2021, Association for the Advancement of Artificial Intelligence (www.aaai.org). All rights reserved.

<sup>1</sup>Our code is available at:  
<https://github.com/tuananhbui89/Crossing-Collaborative-Ensemble>

ative impact of the wrong predictions and ensure the correct predictions of the ensemble model. Moreover, different from other works (Strauss et al., 2017; Pang, Xu, et al., 2019; Kariyappa and Qureshi, 2019) which only consider adversarial examples of the ensemble model, the committee members in our ensemble model are exposed to various divergent adversarial example sets, which inspire them to become gradually more divergent. Interestingly, by strengthening demoting operations, our method is capable to assist better detection of adversarial examples. In brief, our contributions in this work include:

- We propose a simple but efficient collaboration strategy to reduce the transferability among ensemble members.
- We propose two variants of our method: the robust oriented variant, which helps to improve the adversarial robustness and the detection oriented variant, which can detect adversarial examples with high predictive performance.
- We conduct extensive and comprehensive experiments to demonstrate the improvement of our proposed method over the state-of-the-art defense methods.
- We provide a further understanding of the relationship between the transferability and the overall robustness in ensemble learning context.

## Our Proposed Method

In this section, we present our ensemble collaboration strategy, which allows us to collaborate many committee models for improving the ensemble robustness. We start with the definitions and some key properties of secure and insecure sets which later support us in devising promoting and demoting operations for collaborating the committee models to achieve the ensemble robustness. It is worth noting that our ensemble strategy is applicable for ensembling an arbitrary number of committee models; here we focus on presenting the key theories, principles, and operations for the canonical case of ensembling two models for better readability.

### Secure and Insecure Sets

Consider a classification problem on a dataset  $\mathcal{D}$  with  $M$  classes and a pair  $(\mathbf{x}, \mathbf{y})$  that represents a data example  $\mathbf{x}$  and its true label  $\mathbf{y}$  which is sampled from the dataset  $\mathcal{D}$ . Given a model  $f$ , the crucial aim of defense is to make  $f$  robust by giving consistently accurate predictions over a ball,  $\mathcal{B}(\mathbf{x}, \epsilon) := \{\mathbf{x}' : \|\mathbf{x}' - \mathbf{x}\| \leq \epsilon\}$  around a benign data example  $\mathbf{x}$ , for every possible  $\mathbf{x}$  in the dataset  $\mathcal{D}$  and the distortion boundary  $\epsilon$ . To further clarify and motivate our theory, we define

$$\mathcal{B}_{\text{secure}}(\mathbf{x}, \mathbf{y}, f, \epsilon) := \{\mathbf{x}' \in \mathcal{B}(\mathbf{x}, \epsilon) : \operatorname{argmax}_i f_i(\mathbf{x}') = \mathbf{y}\},$$

$$\mathcal{B}_{\text{insecure}}(\mathbf{x}, \mathbf{y}, f, \epsilon) := \{\mathbf{x}' \in \mathcal{B}(\mathbf{x}, \epsilon) : \operatorname{argmax}_i f_i(\mathbf{x}') \neq \mathbf{y}\}.$$

Intuitively, we define a *secure* set  $\mathcal{B}_{\text{secure}}(\mathbf{x}, \mathbf{y}, f, \epsilon)$  as the set of elements in the ball  $\mathcal{B}(\mathbf{x}, \epsilon)$  for which the classifier  $f$  makes the correct prediction. In addition, we define the *insecure* set  $\mathcal{B}_{\text{insecure}}(\mathbf{x}, \mathbf{y}, f, \epsilon)$  as the set of elements in the ball  $\mathcal{B}(\mathbf{x}, \epsilon)$  for which  $f$  predicts differently from the true label  $\mathbf{y}$ . By definition, the secure set

is the complement of the insecure set, and  $\mathcal{B}(\mathbf{x}, \epsilon) = \mathcal{B}_{\text{secure}}(\mathbf{x}, \mathbf{y}, f, \epsilon) \cup \mathcal{B}_{\text{insecure}}(\mathbf{x}, \mathbf{y}, f, \epsilon)$ . It is clear that the aim of improving adversarial robustness is to train the classifier  $f$  in such the way that  $\mathcal{B}_{\text{insecure}}(\mathbf{x}, \mathbf{y}, f, \epsilon)$  is either as small as possible (ideally,  $\mathcal{B}_{\text{insecure}}(\mathbf{x}, \mathbf{y}, f, \epsilon) = \emptyset, \forall \mathbf{x} \in \mathcal{D}$ ) or makes an adversary hard to generate adversarial examples in it. The following simple lemma (see the proof in the supplementary material) shows the connection between those two kinds of sets and the robustness of the ensemble model and facilitates the development of our proposed method.

**Lemma 1.** *Let us define  $f^{\text{en}}(\cdot) = \frac{1}{2}f^1(\cdot) + \frac{1}{2}f^2(\cdot)$  for two given models  $f^1$  and  $f^2$ . If  $f^1$  and  $f^2$  predict an example  $\mathbf{x}$  accurately, we have the following:*

$$\begin{aligned} \text{i) } & \mathcal{B}_{\text{insecure}}(\mathbf{x}, \mathbf{y}, f^{\text{en}}, \epsilon) \subset \mathcal{B}_{\text{insecure}}(\mathbf{x}, \mathbf{y}, f^1, \epsilon) \cup \\ & \mathcal{B}_{\text{insecure}}(\mathbf{x}, \mathbf{y}, f^2, \epsilon). \\ \text{ii) } & \mathcal{B}_{\text{secure}}(\mathbf{x}, \mathbf{y}, f^1, \epsilon) \cap \mathcal{B}_{\text{secure}}(\mathbf{x}, \mathbf{y}, f^2, \epsilon) \subset \\ & \mathcal{B}_{\text{secure}}(\mathbf{x}, \mathbf{y}, f^{\text{en}}, \epsilon). \end{aligned}$$

### Dual Collaborative Ensemble

**Transferring Flow.** Consider the canonical case of an ensemble consisting of two models:  $f^{\text{en}}(\cdot) = \frac{1}{2}f^1(\cdot) + \frac{1}{2}f^2(\cdot)$ , where  $f^{\text{en}}$  is the ensemble model and  $\{f^1, f^2\}$  is the set of ensemble committee (or the committee). Based on the definitions of secure and insecure sets, an arbitrary adversarial example  $\mathbf{x}_a$  must lie in one of four subsets as shown in Table 1. Let us further clarify these subsets. In the first subset  $S_{11} = \mathcal{B}_{\text{secure}}(\mathbf{x}, \mathbf{y}, f^1, \epsilon) \cap \mathcal{B}_{\text{secure}}(\mathbf{x}, \mathbf{y}, f^2, \epsilon)$ , the example  $\mathbf{x}_a$  is predicted correctly by both models, hence also by the ensemble model  $f^{\text{en}}$  (Lemma 1 (ii)). The subsets  $S_{10}, S_{01}$  are the intersection of a secure set of one model and an insecure set of another model, hence an example of two sets is predicted correctly by one model and incorrectly by the other. Lastly, in the subset  $S_{00} = \mathcal{B}_{\text{insecure}}(\mathbf{x}, \mathbf{y}, f^1, \epsilon) \cap \mathcal{B}_{\text{insecure}}(\mathbf{x}, \mathbf{y}, f^2, \epsilon)$ , both models offer predictions other than the true label, but there is also no guarantee that their incorrect predictions are in the same class. There is still a chance that the incorrect prediction in subset  $S_{10}, S_{01}$  dominates the correct ones, which leads to the incorrect prediction on average. Therefore, the insecure region of the overall ensemble should be related to the union  $S_{10} \cup S_{01} \cup S_{00}$  or the total volume (i.e.,  $|S_{10}| + |S_{01}| + |S_{00}|$ ) of the subsets  $S_{10}, S_{01}, S_{00}$ .

As the result, to obtain a robust ensemble model, we need to maintain the subset  $S_{00}$  as small as possible, which is in turn equivalent to making the insecure regions of the two models as disjoint as much as possible (i.e., concurred with Lemma 1 (i)). For the data points in either  $S_{10}$  or  $S_{01}$ , we need to increase the chance that the correct predictions dominate the incorrect ones. Our approach is to encourage adversarial examples inside  $S_{00}$  to move to the subsets  $S_{10}, S_{01}$  during the course of training, and those of  $S_{10}, S_{01}$  to move to the subset  $S_{11}$ . We term this movement as the *transferring flow*, which is described in Table 1. In what follows, we present how to implement the transferring flow for our ensemble model.

**Promoting Adversarial Robustness (PO).** We refer to promoting adversarial robustness as an operation to lever-

Table 1: Four subsets of the ensemble model and the transferring flow (arrows)

	$\mathbf{x}_a \in \mathcal{B}_{\text{secure}}(\mathbf{x}, \mathbf{y}, f^1, \epsilon)$		$\mathbf{x}_a \in \mathcal{B}_{\text{insecure}}(\mathbf{x}, \mathbf{y}, f^1, \epsilon)$
$\mathbf{x}_a \in \mathcal{B}_{\text{secure}}(\mathbf{x}, \mathbf{y}, f^2, \epsilon)$	$S_{11}$	$\leftarrow$	$S_{01}$
	$\uparrow$		$\uparrow$
$\mathbf{x}_a \in \mathcal{B}_{\text{insecure}}(\mathbf{x}, \mathbf{y}, f^2, \epsilon)$	$S_{10}$	$\leftarrow$	$S_{00}$

age the information of an example  $\mathbf{x}_a^i$  (adversarial example of model  $f^i$ ) for improving the robustness of a model  $f^j$  ( $i, j$  can be different). There are several adversarial defense methods that can be applied to promote adversarial robustness, notably (Madry et al., 2018; Hongyang Zhang et al., 2019; Qin et al., 2019). In this work, to promote the adversarial robustness of a given adversarial example  $\mathbf{x}_a^i$  w.r.t the model  $f^j$ , we use adversarial training (Madry et al., 2018) by minimizing the cross-entropy loss w.r.t the true label as  $\min \mathcal{C}(f^j(\mathbf{x}_a^i), \mathbf{y})$ . After undertaking this PO,  $\mathbf{x}_a^i$  is expected to move to the secure set  $\mathcal{B}_{\text{secure}}(\mathbf{x}, \mathbf{y}, f^j, \epsilon)$ . We introduce two types of PO: direct PO (dPO) when  $i = j$  and crossing PO (cPO) when  $i \neq j$ .

**Demoting Adversarial Robustness (DO).** In contrast to promoting adversarial robustness, we refer to demoting adversarial robustness as an operation to sacrifice the robustness of a model for an example  $\mathbf{x}_a^i$  (adversarial example of model  $f^i$ ). Here, we demote the adversarial robustness of a given adversarial example  $\mathbf{x}_a^i$  w.r.t the model  $f^j$  by  $\max \mathcal{H}(f^j(\mathbf{x}_a^i))$  where  $\mathcal{H}$  is the entropy. Without any further knowledge, the prediction is likely uniformly distributed, hence the example  $\mathbf{x}_a^i$  likely falls into the insecure set  $\mathcal{B}_{\text{insecure}}(\mathbf{x}, \mathbf{y}, f^j, \epsilon)$  instead of the secure set  $\mathcal{B}_{\text{secure}}(\mathbf{x}, \mathbf{y}, f^j, \epsilon)$ .

**Collaboration of the Promoting and Demoting Operations.** We now present how to coordinate PO/DO to enforce the transferring flow for enhancing the adversarial robustness of the ensemble model in the canonical case of a committee of two members  $\{f^1, f^2\}$ , parameterized by  $\theta_1$  and  $\theta_2$ . Let  $\mathbf{x}_a^1$  and  $\mathbf{x}_a^2$  be white-box adversarial examples of  $f^1$  and  $f^2$  respectively. With a strong adversary, we can assume that  $\mathbf{x}_a^1 \in \mathcal{B}_{\text{insecure}}(\mathbf{x}, \mathbf{y}, f^1, \epsilon)$  (i.e.,  $\mathbf{x}_a^1 \in S_{01} \cup S_{00}$ ) and  $\mathbf{x}_a^2 \in \mathcal{B}_{\text{insecure}}(\mathbf{x}, \mathbf{y}, f^2, \epsilon)$  (i.e.,  $\mathbf{x}_a^2 \in S_{10} \cup S_{00}$ ). For ease of comprehensibility, we present the treatment for  $\mathbf{x}_a^1$  and the same treatment is applied to  $\mathbf{x}_a^2$ . To strengthen model  $f^1$ , we always use  $\mathbf{x}_a^1$  to promote the robustness of model  $f^1$  by minimizing the cross-entropy loss  $\mathcal{C}(f^1(\mathbf{x}_a^1), \mathbf{y})$  (i.e., flow  $S_{01} \Rightarrow S_{11}$  or  $S_{00} \Rightarrow S_{10}$ ). Meanwhile, we consider two cases of  $\mathbf{x}_a^1$  w.r.t model  $f^2$ : i) being correctly predicted by  $f^2$  (i.e.,  $\mathbf{x}_a^1 \in S_{01}$ ) and ii) being incorrectly predicted by  $f^2$  (i.e.,  $\mathbf{x}_a^1 \in S_{00}$ ). For the first case, we use  $\mathbf{x}_a^1$  to promote model  $f^2$  to make sure  $\mathbf{x}_a^1$  stays in the secure set of model  $f^2$  (i.e.,  $S_{11} \cup S_{01}$ ). For the second case, we demote  $\mathbf{x}_a^1$  w.r.t  $f^2$  by maximizing the entropy  $\mathcal{H}(f^2(\mathbf{x}_a^1))$  in order to keep  $\mathbf{x}_a^1$  in the insecure set of model  $f^2$  (i.e.,  $S_{10} \cup S_{00}$ ).

Therefore, with the collaboration of two models  $f^1$  and  $f^2$  on the same example  $\mathbf{x}_a^1$ , we deploy either flow  $S_{01} \Rightarrow S_{11}$  or  $S_{00} \Rightarrow S_{10}$  depending on the scenario of  $\mathbf{x}_a^1$ . It is worth noting that DO encourages  $f^2(\mathbf{x}_a^1)$  to be close to the uniform prediction, hence causing a minimal effect on the en-

Table 2: Promoting and demoting operations for the transferring flow

Scenario	$f^1$	$f^2$
$\mathbf{x}_a^1 \in S_{01}$	$\min \mathcal{C}(f^1(\mathbf{x}_a^1), \mathbf{y})$	$\min \mathcal{C}(f^2(\mathbf{x}_a^1), \mathbf{y})$
$\mathbf{x}_a^1 \in S_{00}$	$\min \mathcal{C}(f^1(\mathbf{x}_a^1), \mathbf{y})$	$\max \mathcal{H}(f^2(\mathbf{x}_a^1))$
$\mathbf{x}_a^2 \in S_{10}$	$\min \mathcal{C}(f^1(\mathbf{x}_a^2), \mathbf{y})$	$\min \mathcal{C}(f^2(\mathbf{x}_a^2), \mathbf{y})$
$\mathbf{x}_a^2 \in S_{00}$	$\max \mathcal{H}(f^1(\mathbf{x}_a^2))$	$\min \mathcal{C}(f^2(\mathbf{x}_a^2), \mathbf{y})$

semble prediction  $f^{\text{en}}(\mathbf{x}_a^1)$ . As a consequence,  $f^{\text{en}}(\mathbf{x}_a^1) = \frac{1}{2}(f^1(\mathbf{x}_a^1) + f^2(\mathbf{x}_a^1))$  is dominated by  $f^1(\mathbf{x}_a^1)$ , which likely offers a correct prediction via the corresponding PO:  $\min \mathcal{C}(f^1(\mathbf{x}_a^1), \mathbf{y})$ . We summarize the PO/DO to deploy the transferring flow in Table 2.

The objective functions for model  $f^1$  and  $f^2$  to deploy the transferring flow are:

$$\begin{aligned} \mathcal{L}(\mathbf{x}, \mathbf{y}, \theta_1) &= \mathcal{C}(f^1(\mathbf{x}), \mathbf{y}) + \mathcal{C}(f^1(\mathbf{x}_a^1), \mathbf{y}) \\ &\quad + \lambda_{pm} \mathbb{I}(f^1(\mathbf{x}_a^2), \mathbf{y}) \mathcal{C}(f^1(\mathbf{x}_a^2), \mathbf{y}) \\ &\quad - \lambda_{dm} (1 - \mathbb{I}(f^1(\mathbf{x}_a^2), \mathbf{y})) \mathcal{H}(f^1(\mathbf{x}_a^2)), \end{aligned} \quad (1)$$

$$\begin{aligned} \mathcal{L}(\mathbf{x}, \mathbf{y}, \theta_2) &= \mathcal{C}(f^2(\mathbf{x}), \mathbf{y}) + \mathcal{C}(f^2(\mathbf{x}_a^2), \mathbf{y}) \\ &\quad + \lambda_{pm} \mathbb{I}(f^2(\mathbf{x}_a^1), \mathbf{y}) \mathcal{C}(f^2(\mathbf{x}_a^1), \mathbf{y}) \\ &\quad - \lambda_{dm} (1 - \mathbb{I}(f^2(\mathbf{x}_a^1), \mathbf{y})) \mathcal{H}(f^2(\mathbf{x}_a^1)). \end{aligned} \quad (2)$$

where  $\lambda_{pm}$  and  $\lambda_{dm}$  are the hyper-parameters for promoting and demoting effects, respectively, and  $\mathbb{I}(f^1(\mathbf{x}_a^2), \mathbf{y})$  is the indicator to indicate whether  $\mathbf{x}_a^2$  is predicted correctly (i.e.,  $\mathbb{I} = 1$ , hence  $\mathbf{x}_a^2 \in S_{10}$ ) or incorrectly (i.e.,  $\mathbb{I} = 0$ , hence  $\mathbf{x}_a^2 \in S_{00}$ ) by  $f^1$ , which helps to switch on/off the cPO/DO for model  $f^1$ .

For the final objective function, we approximate the hard indicator  $\mathbb{I}(f^1(\mathbf{x}_a^2), \mathbf{y})$  by the soft version  $f_y^1(\mathbf{x}_a^2) = p(\mathbf{y} | \mathbf{x}_a^2, f^1)$ , which represents the probability the model  $f^1$  assigning  $\mathbf{x}_a^2$  to the label  $\mathbf{y}$ . We hence arrive at the following objective functions for both  $f^1$  and  $f^2$ , respectively.

$$\begin{aligned} \mathcal{L}(\mathbf{x}, \mathbf{y}, \theta_1) &= \mathcal{C}(f^1(\mathbf{x}), \mathbf{y}) + \mathcal{C}(f^1(\mathbf{x}_a^1), \mathbf{y}) \\ &\quad + \lambda_{pm} f_y^1(\mathbf{x}_a^2) \mathcal{C}(f^1(\mathbf{x}_a^2), \mathbf{y}) \\ &\quad - \lambda_{dm} (1 - f_y^1(\mathbf{x}_a^2)) \mathcal{H}(f^1(\mathbf{x}_a^2)), \end{aligned} \quad (3)$$

$$\begin{aligned} \mathcal{L}(\mathbf{x}, \mathbf{y}, \theta_2) &= \mathcal{C}(f^2(\mathbf{x}), \mathbf{y}) + \mathcal{C}(f^2(\mathbf{x}_a^2), \mathbf{y}) \\ &\quad + \lambda_{pm} f_y^2(\mathbf{x}_a^1) \mathcal{C}(f^2(\mathbf{x}_a^1), \mathbf{y}) \\ &\quad - \lambda_{dm} (1 - f_y^2(\mathbf{x}_a^1)) \mathcal{H}(f^2(\mathbf{x}_a^1)). \end{aligned} \quad (4)$$

We note that in our implementation, the soft indicators  $f_y^1(\mathbf{x}_a^2)$  and  $f_y^2(\mathbf{x}_a^1)$  are used as values by performing a stopping gradient to prevent the back-propagation process to go inside them for further updating  $f^1$  and  $f^2$ .

## Crossing Collaborative Ensemble

We now extend our collaboration strategy to enable us to ensemble many individual members, which we term as a *Crossing Collaborative Ensemble (CCE)*. Specifically, given an ensemble of  $N$  members  $f^{\text{en}}(\cdot) = \frac{1}{N} \sum_{n=1}^N f^n(\cdot)$  parameterized by  $\theta_n$ , the loss function for a model  $f^n, n \in [1, N]$  as follow:

$$\begin{aligned} \mathcal{L}^n(\mathbf{x}, \mathbf{y}, \theta_n) &= \mathcal{C}(f^n(\mathbf{x}), \mathbf{y}) + \mathcal{C}(f^n(\mathbf{x}_a^n), \mathbf{y}) \\ &+ \frac{1}{N-1} \sum_{i \neq n} \left( \lambda_{pm} f_y^n(\mathbf{x}_a^i) \mathcal{C}(f^n(\mathbf{x}_a^i), \mathbf{y}) \right. \\ &\left. - \lambda_{dm} \left( 1 - f_y^n(\mathbf{x}_a^i) \right) \mathcal{H} \left( f^n(\mathbf{x}_a^i) \right) \right). \end{aligned} \quad (5)$$

It appears from the above loss that we encourage each individual model to (i) minimize the loss of the adversarial example itself for improving its robustness (dPO) and (ii) promoting or demoting its robustness (cPO/DO) with other adversarial examples depending on the soft indicator.

**Connections to Traditional Ensemble Learning.** Firstly, in our method,  $N$  members  $\{f^n\}$  are reinforced with the joint of  $N + 1$  data sources: clean data  $\{\mathbf{x}\}$  and  $N$  adversarial examples  $\{\mathbf{x}_a^n\}_{n=1}^N$ . However, depending on different scenarios, they have the same task (PO-PO) or opposite tasks (PO-DO) on the same adversarial set  $\{\mathbf{x}_a^n\}$ . Our approach can be linked to the bagging technique in the literature, in which each classifier was trained on different sets of data. Secondly, by assigning opposite tasks for ensemble members, our method produces a negative correlation which was described in (Yong Liu and Yao, 1999; Kuncheva and Whitaker, 2003; Bagnall, Bunescu, and Stewart, 2017). It has been claimed that negative relationship among ensemble members can further improve the ensemble accuracy better than the independent correlation.

## Experiments

In this section, we first introduce the experimental setting for adversarial defenses and attackers followed by an extensive evaluation to compare our method with state-of-the-art adversarial defenses. We show that our method surpasses these methods for common benchmark datasets. Next, we provide an ablation study to understand the transferability among ensemble members of adversarial examples. Finally, we show that our method not only detects adversarial examples accurately and consistently but also predicts benign examples with a significant improvement.

### Experimental Setting

**General Setting.** We use CIFAR10 and CIFAR100 as the benchmark datasets in our experiment.<sup>2</sup> Both datasets have 50,000 training images and 10,000 test images. The inputs were normalized to  $[0, 1]$ . We apply random horizontal flips and random shifts with scale 10% for data augmentation as used in (Pang, Xu, et al., 2019). We use both standard CNN architecture and ResNet architecture (K. He et al., 2016) in our experiment. The architecture and training setting for each dataset are provided in our supplementary material.

<sup>2</sup>Recently, (Tsipras et al., 2020) found the labeling issue in the ImageNet dataset, which highly affects the fairness of robustness evaluation on this dataset.

**Crafting Adversarial Examples for Defenders.** In our experiments, we use PGD  $\{k, \epsilon, \eta, l_\infty\}$  as the common adversary to generate adversarial examples for the adversarial training of all defenders where  $k$  is the iteration steps,  $\epsilon$  is the distortion bound and  $\eta$  is the step size. Specifically, the configuration for the CIFAR10 dataset is  $k = 10, \epsilon = 8/255, \eta = 2/255$  and that for the CIFAR100 dataset is  $k = 10, \epsilon = 0.01, \eta = 0.001$ . For the CIFAR10 dataset with ResNet architecture, we use the same setting in (Pang, Xu, et al., 2019) which is  $k = 10, \epsilon \sim U(0.01, 0.05), \eta = \epsilon/10$ .

**Baseline Methods.** Because the model capacity has significant impact on the inference performance, therefore, for a fair comparison, we compare our method with the start-of-the-art ensemble-based method, i.e., ADV-EN (Madry et al., 2018) and ADP (Pang, Xu, et al., 2019), which have the same number of committee members and also the member’s architecture. More specifically, ADV-EN is the variant of PGD adversarial training method (ADV) in the context of ensemble learning, in which the entire ensemble model is treated as one unified model applied with adversarial training. We also compare with the ADV method which is adversarial training on a single model. For ADP, we choose the best setting  $ADP_{2,0.5}$  with adversarial version, which was reported in the paper (Pang, Xu, et al., 2019), and use the official code.<sup>3</sup>

Throughout our experiments, we use two variants of our method: (i) Robustness Mode (i.e., CCE-RM) for which we set  $\lambda_{pm} = \lambda_{dm} = 1$  and (ii) Detection Mode (i.e., CCE-DM) for which we disable cPO ( $\lambda_{pm} = 0$ ) and strengthen DO (i.e.,  $\lambda_{dm} = 5$ ).

**Attack Setting.** We use different state-of-the-art attacks to evaluate the defense methods including:

(i) **Gradient based attacks** (with *cleverhans*<sup>4</sup> lib). We use PGD (Madry et al., 2018), the Basic Iterative Method (BIM) (Kurakin, I. J. Goodfellow, and S. Bengio, 2017) and the Momentum Iterative Method (MIM) (Dong et al., 2018). They share the same hyper-parameters configuration, i.e.,  $\{k, \epsilon, \eta\}$ , which is described in each individual experiment.

(ii) **B&B attack** (Brendel et al., 2019) (with *foolbox*<sup>5</sup> lib) which is a decision based attack. We argue that the B&B attack setting in the paper of (Tramer et al., 2020) may not be appropriate to evaluate the ADP method. It is because the ADP method used PGD ( $\epsilon \sim U(0.01, 0.05), k = 10$ ) for its adversarial training, while B&B attack used PGD ( $\epsilon = 0.15, k = 20$ ) as an initialized attack which is much stronger than the defense capacity. More specifically, the initialized PGD attack alone can reduce the accuracy to 0.1%. Therefore, B&B attack contributes very little to the final attack performance. To have a fair evaluation, we use two initialized attacks with lower strength: PGD1 ( $\epsilon = 8/255, \eta = 2/255, k = 20$ ) and PGD2 ( $\epsilon = 16/255, \eta = 2/255, k = 20$ ) then apply B&B attack with 100 steps and repeat for three times. It is worth noting that, PGD2 is still much stronger than the defense capacity, however, we use this set-

<sup>3</sup><https://github.com/P2333/Adaptive-Diversity-Promoting>

<sup>4</sup><https://github.com/tensorflow/cleverhans>

<sup>5</sup><https://foolbox.readthedocs.io/en/stable/>

Table 3: Robustness evaluation on the CIFAR10 dataset with ResNet architecture. For the PGD attack, we use  $\epsilon = 8/255, \eta = 2/255$ . (\*) The low robust accuracies (even with standard method ADV) because the attack strength of PGD2 is double of the defense capacity, which makes the adversarial examples to be recognizable.

Attack	ADV <sub>1</sub>	ADV-EN <sub>2</sub>	ADP <sub>2</sub>	CCE-RM <sub>2</sub>	ADV-EN <sub>3</sub>	ADP <sub>3</sub>	CCE-RM <sub>3</sub>
Non-att (Nat. acc.)	83.9	85.3	<b>85.3</b>	84.5	86.1	<b>86.2</b>	84.9
PGD $k = 250$	41.4	42.8	44.2	<b>45.8</b>	43.8	45.1	<b>48.6</b>
BIM $k = 250$	41.5	42.9	44.1	<b>45.8</b>	44.0	45.2	<b>48.8</b>
MIM $k = 250$	41.9	43.3	44.8	<b>46.3</b>	44.5	45.7	<b>49.1</b>
B&B (wPGD1)	37.0	38.3	37.3	<b>42.2</b>	39.3	38.3	<b>44.2</b>
B&B (wPGD2)*	4.9	2.9	3.9	<b>6.0</b>	4.2	4.3	<b>7.1</b>
SPSA	50.0	53.5	52.8	<b>56.2</b>	53.8	53.9	<b>56.6</b>
Auto-Attack	16.1	18.5	17.3	<b>18.8</b>	18.4	17.6	<b>20.8</b>

ting to mimic the evaluation in the paper of (Tramer et al., 2020).

(iii) **Auto-Attack** (Croce and Hein, 2020) (with the official implementation<sup>6</sup>) which is an ensemble based attack. We use  $\epsilon = 8/255$  for the CIFAR10 dataset and  $\epsilon = 0.01$  for the CIFAR100 dataset, both with standard version which is an ensemble of four different attacks.

(iv) **SPSA attack** (Uesato et al., 2018) (with *cleverhans* lib) which is a gradient-free optimization method. We use  $\epsilon = 8/255$  for the CIFAR10 dataset and  $\epsilon = 0.01$  for the CIFAR100 dataset, both with 50 steps.

The distortion metric we use in our experiments is  $l_\infty$  for all measures. We use the full test set for the attacks (i) and 1000 test samples for the attacks (ii-iv).

## Robustness Evaluation

We conduct extensive experiments on the CIFAR10 and CIFAR100 datasets to compare our method with the other methods. We consider the ensemble of both two and three committee members (denoted by a subscript number in each method). It can be observed from the experimental results in Table [3, 4, 5] that:

(i) There is a gap of 2%~3% when comparing ADV-EN<sub>3</sub> with ADV<sub>1</sub> showing that increasing model capacity (by increasing number of ensemble member) can improve the robustness of the model.

(ii) There is a gap of 3%~4% between ADP<sub>3</sub> and ADV<sub>1</sub>, and especially, a gap of 7%~8% when comparing our CCE-RM<sub>3</sub> with ADV<sub>1</sub>, which shows the potential of the ensemble learning to tackle with the adversarial attacks.

(iii) With the same model capacity, our CCE-RM is consistently the best with all attacks and in some attacks, ours surpasses other baselines in a large margin (4%~5%).

(iv) There is a gap of 3% between CCE-RM<sub>3</sub> and CCE-RM<sub>2</sub>, which is larger than the gap of 1% between ADP<sub>3</sub> and ADP<sub>2</sub> or that of ADV-EN<sub>3</sub> and ADV-EN<sub>2</sub>, showing that our method collaborates members better and gets more benefit from ensembling more committee members.

The effectiveness of adversarial training method depends on the diversity (or the hardness) of the adversarial examples (Madry et al., 2018). Fort et al. (2019) found that differently initializing members' parameters, even with the same train-

<sup>6</sup><https://github.com/fra31/auto-attack>

Table 4: Robustness evaluation on the CIFAR10 dataset with standard CNN architecture. We use  $\epsilon = 8/255, \eta = 2/255$ . Note that *mulA* represents for multiple-targeted attack by adversary  $\mathcal{A}$ .

Attack	ADV <sub>1</sub>	ADV-EN <sub>2</sub>	ADP <sub>2</sub>	CCE-RM <sub>2</sub>	ADV-EN <sub>3</sub>	ADP <sub>3</sub>	CCE-RM <sub>3</sub>
Non-att (Nat. acc.)	75.7	76.0	75.9	<b>76.0</b>	<b>76.7</b>	76.6	75.7
PGD $k = 100$	38.0	39.7	42.2	<b>44.7</b>	40.8	43.9	<b>46.8</b>
BIM $k = 100$	38.2	39.7	42.2	<b>44.9</b>	40.8	43.8	<b>46.8</b>
MIM $k = 100$	38.5	40.5	42.4	<b>45.4</b>	41.3	44.2	<b>47.2</b>
mul-PGD $k = 20$	26.0	27.7	27.8	<b>31.9</b>	28.3	32.4	<b>36.9</b>
mul-BIM $k = 20$	25.9	27.2	27.2	<b>31.6</b>	27.7	29.8	<b>34.1</b>
mul-MIM $k = 20$	26.2	28.1	28.3	<b>32.3</b>	29.0	30.7	<b>34.6</b>
SPSA	40.6	44.3	41.5	<b>45.2</b>	45.1	46.1	<b>47.5</b>
Auto-Attack	25.1	25.0	24.4	<b>29.9</b>	25.5	28.1	<b>31.9</b>

Table 5: Robustness evaluation on the CIFAR100 dataset with standard CNN architecture. We use  $\epsilon = 0.01, \eta = 0.001$ . Note that *mulA* represents for multiple-targeted attack by adversary  $\mathcal{A}$ .

Attack	ADV <sub>1</sub>	ADV-EN <sub>2</sub>	ADP <sub>2</sub>	CCE-RM <sub>2</sub>	ADV-EN <sub>3</sub>	ADP <sub>3</sub>	CCE-RM <sub>3</sub>
Non-att (Nat. acc.)	40.8	41.4	48.0	<b>53.4</b>	40.8	52.6	<b>54.4</b>
PGD $k = 100$	26.8	29.7	30.9	<b>35.3</b>	32.8	36.2	<b>39.5</b>
BIM $k = 100$	26.9	29.1	31.0	<b>35.2</b>	32.8	36.2	<b>39.4</b>
MIM $k = 100$	27.0	29.0	30.8	<b>35.3</b>	32.9	36.1	<b>39.6</b>
mul-PGD $k = 20$	16.4	15.8	20.1	<b>24.2</b>	16.6	24.8	<b>28.4</b>
mul-BIM $k = 20$	15.9	15.5	19.4	<b>23.7</b>	16.3	24.5	<b>28.1</b>
mul-MIM $k = 20$	16.7	16.1	20.3	<b>24.1</b>	16.8	25.1	<b>28.6</b>
SPSA	25.6	25.5	24.1	<b>31.8</b>	26.0	32.5	<b>35.0</b>
Auto-Attack	15.3	15.1	14.8	<b>21.9</b>	15.8	23.0	<b>25.9</b>

ing data, can end up with different local optimal in the solution space. Therefore, the potential of ensemble learning (in the remark ii) can be explained by the fact that the adversarial space of an ensemble model  $\mathcal{B}_{\text{insecure}}(\mathbf{x}, \mathbf{y}, f^{\text{en}}, \epsilon)$  is more diverse than that of a single model  $\mathcal{B}_{\text{insecure}}(\mathbf{x}, \mathbf{y}, f, \epsilon)$ .

Our advantages over others (in the remark iii, iv) can be explained by the fact that our proposed method encourages the diversity of its committee members. Specifically it can be elaborated on with the following three key points. Firstly, while other ensemble-based defenses use the adversarial examples of the entire ensemble  $\mathbf{x}_a^{\text{en}} \sim \mathcal{B}_{\text{insecure}}(\mathbf{x}, \mathbf{y}, f^{\text{en}}, \epsilon)$ , our method makes use of the broader joint adversarial space  $\mathbf{x}_a^i \sim \mathcal{B}_{\text{insecure}}(\mathbf{x}, \mathbf{y}, f^i, \epsilon)$  (Lemma 1 (i)). Secondly, each member has different loss landscape (Fort, Hu, and Lakshminarayanan, 2019), in addition with the randomness of an adversary (e.g., random starting points in PGD), each member has its individual adversarial set (partly collapsed as shown in the next experiment). Therefore, similar with the bagging technique, by promoting each member with its adversarial examples independently, we can increase the diversity of the joint adversarial space. Last but not least, inspired from traditional ensemble learning (Yong Liu and Yao, 1999), by elegantly collaborating PO and DO, we encourage the negative correlation among ensemble members, therefore, further improve the diversity of the joint adversarial space.

## Transferability among Ensemble Members

The transferability is a phenomenon when adversarial examples generated to attack a specific model also mislead other models trained for the same task. In the ensemble learning context, adversarial examples which are transferred well among members will likely fool the entire ensemble. There-

fore, reducing the transferability among members is a principled approach to achieve better robustness as claimed in the previous works (Pang, Xu, et al., 2019; Kariyappa and Qureshi, 2019). In this sub-section, we provide a further understanding of the transferability to the overall robustness and show the impact of the transferring flow.

We first summarize the experiments setting. The experiments are conducted on the CIFAR10 dataset with an ensemble of two members under PGD attack with  $k = 20$ ,  $\epsilon = 8/255$ ,  $\eta = 2/255$ . The results are reported in Table 6. CCE-Base is our model which disables the crossing PO and DO by setting  $\lambda_{pm} = \lambda_{dm} = 0$ .  $a^{(i,j)}$  represents for the robust accuracy when adversarial examples  $\{x_a^i\}$  attack model  $f^j$ .  $|S|$  shows the cardinality of a subset  $S$ , i.e., the percentage of the images that go into the subset  $S$ , which can be one of  $\{S_{11}, S_{01}, S_{10}, S_{00}\}$ . From the definition of the transferability as mentioned above, to measure the transferability of adversarial examples  $\{x_a^i\}$ , we can compute the accuracy difference of model  $f^i$  and  $f^j$ ,  $j \neq i$  against the same attack  $\{x_a^i\}$ . The smaller gap implies that adversarial examples  $\{x_a^i\}$  are more transferable. The overall transferability of an ensemble method can be evaluated by the sum the accuracy differences over all its members, i.e.,  $T = a^{(1,2)} - a^{(1,1)} + a^{(2,1)} - a^{(2,2)}$ .

We would like to emphasize some following important empirical observations (Table 6):

1) **The impact of the transferring flow.** It can be observed that the cardinality  $|S_{11}|$  in CCE-RM (39.9%) is larger than that in CCE-Base (36.1%), while the cardinality  $|S_{01}|, |S_{10}|, |S_{00}|$  is smaller than those in CCE-Base which serves as evidence that the adversarial examples are successfully transferred from subsets  $S_{10}, S_{01}, S_{00}$  to subset  $S_{11}$  as we expect. This helps improve the overall robustness of the ensemble model from 43.3% for CCE-Base to 45.5% for CCE-RM.

2) **The transferable space is just a subset of the adversarial space.** By definition, the subset  $S_{00}$  consists of adversarial examples which fools both models  $f^1, f^2$ , therefore,  $S_{00}$  represents for the transferable space of the ensemble model  $f^{en}$ . In fact, the cardinality of  $|S_{00}|$  is smaller than the insecure region of the ensemble model  $f^{en}$  (i.e., the total classification error  $100\% - a^{(en,en)}$ ) in all methods showing that the transferable space cannot represent for the insecure region of the ensemble model  $f^{en}$ , and the former is just the subset of the latter.

3) **Reducing transferability among ensemble members is not enough to improve adversarial robustness.** In fact, the transferability metric  $T$  for CCE-RM is 33.7% which is much smaller than those for ADP and ADV-EN (59.3% and 65.5%, respectively). The smaller value of  $T$  shows that the adversarial examples  $\{x_a^1\}, \{x_a^2\}$  in our method are more transferable than those in ADV-EN and ADP. However, the fact that the overall robustness of our method is significantly better evidently shows that *transferability is not the only factor for improving the robustness*. This is because the robustness of each individual member under a direct attack (i.e.,  $a^{(1,1)}$  or  $a^{(2,2)}$ ) is much lower than our method. In addition, the cardinality  $|S_{11}|$  in our method is 39.9% which is much

Table 6: Evaluation on the transferability among ensemble members on the CIFAR10 dataset.  $\{T, nT, a_{single}\}$  are the metrics of interest.

Model	$a^{(en,en)}$	$a^{(1,1)}$	$a^{(2,2)}$	$ S_{11} $	$ S_{01} $	$ S_{10} $	$ S_{00} $	$T$	$nT$	$a_{single}$
ADV-EN	40.7	31.1	33.2	24.0	17.0	13.0	46.0	65.5	13.3	16.7
ADP	42.9	31.0	33.1	25.7	13.1	11.7	49.5	59.3	7.6	17.2
CCE-RM	45.5	41.7	41.4	39.9	5.2	5.5	49.5	33.7	5.0	5.6
CCE-Base	43.3	40.3	40.5	36.1	6.5	7.2	50.3	36.1	6.4	7.2

bigger than those in ADV-EN (24.0%) and ADP (25.7%).

We provide two additional metrics which are (i)  $nT = 100\% - a^{(en,en)} - |S_{00}|$  to measure the cardinality of *adversarial examples set which successful attack model  $f^{en}$  but non transferable among  $f^1, f^2$*  and (ii)  $a_{single} = a^{(en,en)} - |S_{11}|$  to measure the cardinality of *adversarial examples set which are correctly predicted by only one model either  $f^1$  or  $f^2$  but still being correctly predicted by model  $f^{en}$* . The comparison on the metric  $nT$  in Table 6 shows that most of successful adversarial examples in our method are predicted incorrectly by both members. While the comparison on the metric  $a_{single}$  shows that most of unsuccessful adversarial examples in our method are predicted correctly by both members. The two comparisons demonstrate that our method have better robustness than other methods because (i) the adversarial examples have to fool both ensemble members for a successful attack and (ii) our ensemble model can predict correctly by both members which explains the higher performance.

The remarks (2, 3) further imply that:

*An ensemble model cannot be secure against white-box attacks unless its members are robust against direct attacks (even they are secure against transferred attacks).*

This hypothesis provides more understanding of the correlation between the transferability and the overall robustness of an ensemble model.

## Improving Natural Accuracy and Adversarial Detectability

The parameter  $\lambda_{pm}(\lambda_{dm})$  controls the level of the agreement (disagreement) of models  $\{f^i\}, i \in [1, N]$  and model  $f^j, j \neq i$  on the same adversarial example  $x_a^j$ . By disabling the crossing PO ( $\lambda_{pm} = 0$ ) and strengthening DO (i.e.,  $\lambda_{dm} = 5$ ), our method encourages the disagreement among members on the same data example, therefore, increases the negative correlation among them. This setting of CCE-DM leads to two important properties, which are empirically proved by the experiments below.

**Improving Natural Accuracy.** We compare natural accuracies of two variants: CCE-RM and CCE-DM against the baselines. Table 7 shows that CCE-DM significantly improves natural accuracy of the ensemble model by a large margin. In traditional ensemble learning, the key ingredient to improve natural performance is making ensemble members more diverse (Kuncheva and Whitaker, 2003). By disabling the crossing PO and strengthening DO, CCE-DM variant enforces the diversity more strictly, which explains

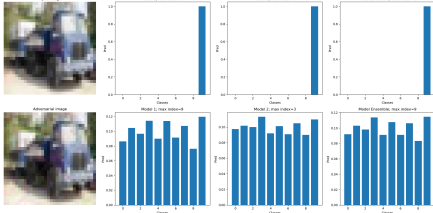


Figure 1: Prediction example in the detection mode. Top/bottom images are benign/adversarial images. Next columns are outputs from  $f^1, f^2, f^{en}$

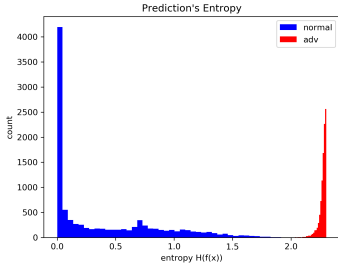


Figure 2: Histogram of prediction entropy in the detection mode

the improvement of the natural performance. This result demonstrates the promising usage of adversarial examples to improve the traditional ensemble learning.

Table 7: Comparison of the natural performance on the CIFAR10 dataset (the subscript number denotes the number members).

Model	ADV-EN	ADP	CCE-RM	CCE-DM
CNN <sub>2</sub>	76.0	75.9	76.0	86.0
CNN <sub>3</sub>	76.7	76.6	75.7	87.2
ResNet <sub>2</sub>	85.3	85.3	84.5	91.0
ResNet <sub>3</sub>	86.1	86.2	84.9	91.6

**Adversarial Detectability.** CCE-DM can distinguish between benign and adversarial examples more easily. It is because the committee members produce a uniform prediction for adversarial examples, while yielding a very high confident prediction for benign examples. For example, as shown in Figure 1, the committee members are highly certain when predicting benign examples, while they provide highly uncertain predictions with high entropy for adversarial examples. The histogram for all images in the test set and their adversarial examples in Figure 2 demonstrate the consistency of this observation over the data distribution.

These results further inspire us to develop a simple yet effective method to detect adversarial examples based on the entropy of the model prediction. Following the evaluation in (Pang, Du, et al., 2018; Pang, Xu, et al., 2019), we try with different thresholds to distinguish the benign and adversarial examples and report the AUC score of each adversarial attack. It is worth noting that, we do not intend to compete

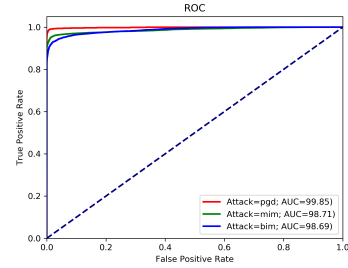


Figure 3: ROC of CCE-RM under multiple types of attack

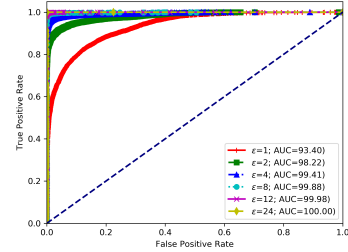


Figure 4: ROC of CCE-RM under multiple attack strengths

with other adversarial detectors but just to show the advantage and flexibility of our CCE. The experiment is on the CIFAR10 dataset with an ensemble of two members. We conduct two evaluations to justify our understanding. First, we study our detection method against three different attacks: PGD, BIM and MIM with the same hyper-parameter setting  $k = 20, \epsilon = 8/255, \eta = 1/255$ . The result in Figure 3 shows that our method can accurately and consistently detect all three kind of attacks. Secondly, we study our detection method on different attack strengths. We use the PGD attack  $k = 20, \eta = 1/255$  and vary the distortion bound  $\epsilon$  from  $1/255$  to  $24/255$ . The result in Figure 4 shows that our method can perform well on a wide range of attack strengths. The adversary is obviously less distinguishable when decreasing its strength. However, our method still obtains a very high AUC score (93.4/100) even under a very weak attack ( $\epsilon = 1/255$ ), in which adversarial images look nearly identical to the original ones.

## Conclusion

In this paper, we explore the use of ensemble-based learning to improve adversarial robustness. In particular, we propose a cross-collaborative strategy by means of enforcing the transferring flow of adversarial examples, thereby implicitly increasing the diversity of adversarial space and improving the robustness of the ensemble. Moreover, our proposed method can be performed in both detection and robustness modes. We conduct extensive and comprehensive experiments to show the improvement of our proposed method on state-of-the-art baselines. We also provide the detailed understanding of the relationship between the transferability and the overall robustness in the ensemble learning context.

**Acknowledgement.** This work was partially supported by the Australian Defence Science and Technology (DST) Group under the Next Generation Technology Fund (NTGF) scheme.

## References

- Athalye, Anish, Nicholas Carlini, and David Wagner (2018). “Obfuscated Gradients Give a False Sense of Security: Circumventing Defenses to Adversarial Examples”. In: *International Conference on Machine Learning*, pp. 274–283.
- Bagnall, Alexander, Razvan Bunescu, and Gordon Stewart (2017). “Training ensembles to detect adversarial examples”. In: *arXiv preprint arXiv:1712.04006*.
- Biggio, Battista et al. (2013). “Evasion attacks against machine learning at test time”. In: *Joint European conference on machine learning and knowledge discovery in databases*. Springer, pp. 387–402.
- Brendel, Wieland et al. (2019). “Accurate, reliable and fast robustness evaluation”. In: *Advances in Neural Information Processing Systems*, pp. 12861–12871.
- Bui, Anh et al. (2020). “Improving Adversarial Robustness by Enforcing Local and Global Compactness”. In: *arXiv preprint arXiv:2007.05123*.
- Carlini, N. and D. Wagner (2017). “Towards evaluating the robustness of neural networks”. In: *2017 IEEE Symposium on Security and Privacy (SP)*. IEEE, pp. 39–57.
- Croce, Francesco and Matthias Hein (2020). “Reliable evaluation of adversarial robustness with an ensemble of diverse parameter-free attacks”. In: *arXiv preprint arXiv:2003.01690*.
- Dong, Yinpeng et al. (2018). “Boosting adversarial attacks with momentum”. In: *Proceedings of the IEEE conference on computer vision and pattern recognition*, pp. 9185–9193.
- Fort, Stanislav, Huiyi Hu, and Balaji Lakshminarayanan (2019). “Deep ensembles: A loss landscape perspective”. In: *arXiv preprint arXiv:1912.02757*.
- Goodfellow, Ian, Yoshua Bengio, and Aaron Courville (2016). *Deep learning*. MIT press.
- Goodfellow, Ian J., Jonathon Shlens, and Christian Szegedy (2015). “Explaining and Harnessing Adversarial Examples”. In: *3rd International Conference on Learning Representations, ICLR 2015, San Diego, CA, USA, May 7-9, 2015, Conference Track Proceedings*. Ed. by Yoshua Bengio and Yann LeCun. URL: <http://arxiv.org/abs/1412.6572>.
- He, Kaiming et al. (2016). “Deep residual learning for image recognition”. In: *Proceedings of the IEEE conference on computer vision and pattern recognition*, pp. 770–778.
- He, Warren et al. (2017). “Adversarial example defense: Ensembles of weak defenses are not strong”. In: *11th {USENIX} Workshop on Offensive Technologies ({WOOT} 17)*.
- Kariyappa, Sanjay and Moinuddin K Qureshi (2019). “Improving adversarial robustness of ensembles with diversity training”. In: *arXiv preprint arXiv:1901.09981*.
- Kuncheva, Ludmila I and Christopher J Whitaker (2003). “Measures of diversity in classifier ensembles and their relationship with the ensemble accuracy”. In: *Machine learning* 51.2, pp. 181–207.
- Kurakin, Alexey, Ian J. Goodfellow, and Samy Bengio (2017). “Adversarial examples in the physical world”. In: *5th International Conference on Learning Representations, ICLR 2017, Toulon, France, April 24-26, 2017, Workshop Track Proceedings*. OpenReview.net. URL: <https://openreview.net/forum?id=HJGU3Rodl>.
- Liu, Xuanqing et al. (2018). “Towards robust neural networks via random self-ensemble”. In: *Proceedings of the European Conference on Computer Vision (ECCV)*, pp. 369–385.
- Liu, Yanpei et al. (2016). “Delving into transferable adversarial examples and black-box attacks”. In: *arXiv preprint arXiv:1611.02770*.
- Liu, Yong and Xin Yao (1999). “Ensemble learning via negative correlation”. In: *Neural networks* 12.10, pp. 1399–1404.
- Madry, Aleksander et al. (2018). “Towards Deep Learning Models Resistant to Adversarial Attacks”. In: *International Conference on Learning Representations*.
- Moosavi-Dezfooli, Seyed-Mohsen, Alhussein Fawzi, and Pascal Frossard (2016). “Deepfool: a simple and accurate method to fool deep neural networks”. In: *Proceedings of the IEEE conference on computer vision and pattern recognition*, pp. 2574–2582.
- Pang, Tianyu, Chao Du, et al. (2018). “Towards robust detection of adversarial examples”. In: *Advances in Neural Information Processing Systems*, pp. 4579–4589.
- Pang, Tianyu, Kun Xu, et al. (2019). “Improving Adversarial Robustness via Promoting Ensemble Diversity”. In: *International Conference on Machine Learning*, pp. 4970–4979.
- Papernot, Nicolas, Patrick McDaniel, and Ian Goodfellow (2016). “Transferability in machine learning: from phenomena to black-box attacks using adversarial samples”. In: *arXiv preprint arXiv:1605.07277*.
- Papernot, Nicolas, Patrick D. McDaniel, et al. (2016). “The Limitations of Deep Learning in Adversarial Settings”. In: *IEEE European Symposium on Security and Privacy, EuroS&P 2016, Saarbrücken, Germany, March 21-24, 2016*. IEEE, pp. 372–387. DOI: 10.1109/EuroSP.2016.36. URL: <https://doi.org/10.1109/EuroSP.2016.36>.
- Qin, Chongli et al. (2019). “Adversarial robustness through local linearization”. In: *Advances in Neural Information Processing Systems*, pp. 13824–13833.
- Shafahi, A. et al. (2019). “Adversarial training for free!” In: *Advances in Neural Information Processing Systems*, pp. 3353–3364.
- Strauss, Thilo et al. (2017). “Ensemble methods as a defense to adversarial perturbations against deep neural networks”. In: *arXiv preprint arXiv:1709.03423*.
- Szegedy, Christian et al. (2014). “Intriguing properties of neural networks”. In: *2nd International Conference on Learning Representations, ICLR 2014, Banff, AB, Canada, April 14-16, 2014, Conference Track Proceedings*. Ed. by Yoshua Bengio and Yann LeCun. URL: <http://arxiv.org/abs/1312.6199>.



- Tramer, Florian et al. (2020). “On adaptive attacks to adversarial example defenses”. In: *Advances in Neural Information Processing Systems* 33, pp. 1633–1645.
- Tramèr, Florian, Alexey Kurakin, et al. (2018). “Ensemble adversarial training: Attacks and defenses”. In: *6th International Conference on Learning Representations, ICLR 2018*.
- Tramèr, Florian, Nicolas Papernot, et al. (2017). “The space of transferable adversarial examples”. In: *arXiv preprint arXiv:1704.03453*.
- Tsipras, Dimitris et al. (2020). “From ImageNet to Image Classification: Contextualizing Progress on Benchmarks”. In: *arXiv preprint arXiv:2005.11295*.
- Uesato, Jonathan et al. (2018). “Adversarial Risk and the Dangers of Evaluating Against Weak Attacks”. In: *International Conference on Machine Learning*, pp. 5025–5034.
- Vaswani, Ashish et al. (2017). “Attention is all you need”. In: *Advances in neural information processing systems*, pp. 5998–6008.
- Xie, Cihang et al. (2020). “Smooth adversarial training”. In: *arXiv preprint arXiv:2006.14536*.
- Zhang, Haichao and Jianyu Wang (2019). “Defense against adversarial attacks using feature scattering-based adversarial training”. In: *Advances in Neural Information Processing Systems*, pp. 1829–1839.
- Zhang, Hongyang et al. (2019). “Theoretically Principled Trade-off between Robustness and Accuracy”. In: *arXiv preprint arXiv:1901.08573*.

## Supplementary materials for “Improving Ensemble Robustness by Collaboratively Promoting and Demoting Adversarial Robustness”

### Proof

**Lemma 2.** *Let us define  $f^{ens}(\cdot) = \frac{1}{2}f^1(\cdot) + \frac{1}{2}f^2(\cdot)$  for two given models  $f^1$  and  $f^2$ . If  $f^1$  and  $f^2$  predict an example  $\mathbf{x}$  accurately, we have the following:*

- i)  $\mathcal{B}_{insecure}(\mathbf{x}, \mathbf{y}, f^{ens}, \epsilon) \subset \mathcal{B}_{insecure}(\mathbf{x}, \mathbf{y}, f^1, \epsilon) \cup \mathcal{B}_{insecure}(\mathbf{x}, \mathbf{y}, f^2, \epsilon)$ .
- ii)  $\mathcal{B}_{secure}(\mathbf{x}, \mathbf{y}, f^1, \epsilon) \cap \mathcal{B}_{secure}(\mathbf{x}, \mathbf{y}, f^2, \epsilon) \subset \mathcal{B}_{secure}(\mathbf{x}, \mathbf{y}, f^{ens}, \epsilon)$ .

*Proof.* It is obvious that Lemma 2 (i) and (ii) are equivalent. We hence need to prove only Lemma 2 (ii). Consider a classification problem on a dataset  $\mathcal{D}$  with  $M$  classes, the true label of  $\mathbf{x}$  is  $\mathbf{y} \in \{1, 2, \dots, M\}$  and let  $\mathbf{x}' \in \mathcal{B}_{secure}(\mathbf{x}, \mathbf{y}, f^1, \epsilon) \cap \mathcal{B}_{secure}(\mathbf{x}, \mathbf{y}, f^2, \epsilon)$ . Since  $f^1$  and  $f^2$  predict  $\mathbf{x}'$  correctly with the label  $\mathbf{y}$ , we then have:

$$\begin{aligned} f_y^1(\mathbf{x}') &\geq f_j^1(\mathbf{x}'), \forall j \in \{1, 2, \dots, M\}, \\ f_y^2(\mathbf{x}') &\geq f_j^2(\mathbf{x}'), \forall j \in \{1, 2, \dots, M\}. \end{aligned}$$

This follows that

$$f_y^{ens}(\mathbf{x}') \geq f_j^{ens}(\mathbf{x}'), \forall j \in \{1, 2, \dots, M\},$$

which means

$$\mathbf{x}' \in \mathcal{B}_{secure}(\mathbf{x}, \mathbf{y}, f^{ens}, \epsilon).$$

□

### Related works

In this section we introduce the most related works to our approach including adversarial training and ensemble-based methods.

#### Adversarial Training.

Adversarial training (ADV) can be traced back to (I. J. Goodfellow, Shlens, and Szegedy, 2015), in which a model becomes more robust by incorporating its adversarial examples into training data. Given a model  $f$ , a benign example pair  $(\mathbf{x}, \mathbf{y})$  and an adversarial example  $\mathbf{x}_a$ , the objective function of ADV as:

$$\mathcal{L}_{AT}(\mathbf{x}, \mathbf{x}_a, \mathbf{y}) = \mathcal{L}(f(\mathbf{x}), \mathbf{y}) + \mathcal{L}(f(\mathbf{x}_a), \mathbf{y})$$

Although many defense models were broken by (Athalye, Nicholas Carlini, and David Wagner, 2018) or gave a false sense of robustness because of the obfuscated gradient, the adversarial training (Madry et al., 2018) was among the few that were resilient against attacks. Many ADV’s variants have been developed including but not limited to: (1) difference in the choice of adversarial examples, e.g., the worst-case examples (I. J. Goodfellow, Shlens, and Szegedy, 2015) or most divergent examples (Hongyang Zhang et al., 2019), (2) difference in the searching of adversarial examples, e.g., non-iterative FGSM, Rand FGSM with random initial point or PGD with multiple iterative gradient descent

steps (Madry et al., 2018; Shafahi et al., 2019), (3) difference in additional regularizations, e.g., adding constraints in the latent space (Haichao Zhang and Wang, 2019; Bui et al., 2020), (4) difference in model architecture, e.g., activation function (Xie et al., 2020) or ensemble models (Pang, Xu, et al., 2019).

### Ensemble-based Defenses.

Recent works (Tramèr, Kurakin, et al., 2018; Kariyappa and Qureshi, 2019) shows that ensemble adversarial trained models can reduce the dimensionality of adversarial subspace (Tramèr, Papernot, et al., 2017). There are different approaches, however, the key ingredient of their stories is reducing the transferability of adversarial examples between members. In (Tramèr, Kurakin, et al., 2018), the authors used the crafted perturbations from static pretrained models as augmented data to decouple the generation process of adversarial examples of target model. However, as reported in (Tramèr, Kurakin, et al., 2018), this method was designed for black-box attacks, thus still vulnerable to white-box attacks. In (Kariyappa and Qureshi, 2019), robustness was achieved by aligning the gradient of committee members to be diametrically opposed, hence reducing the shared adversarial spaces, or the transferability. However, attempting to achieve gradient alignment is unreliable for high-dimensional datasets and it is difficult to extend for ensemble with more than two committee members. More recently, (Pang, Xu, et al., 2019) proposed to promote the diversity of non-maximal predictions of the committee members (i.e., the diversity among softmax probabilities except the highest ones) to reduce the adversarial transferability among them. The adaptive diversity promoting (ADP) regularizer as:  $ADP_{\alpha,\beta}(\mathbf{x}, \mathbf{y}) = \alpha \mathcal{H}(\mathcal{F}) + \beta \log(\mathbb{E}\mathbb{D})$ , where  $\mathcal{H}(\mathcal{F})$  is the Shannon entropy of the ensemble prediction and  $\log(\mathbb{E}\mathbb{D})$  is the logarithm of the ensemble diversity. As reported in their paper, ADP can cooperate with adversarial training to increase the robustness. In this case, the objective function of ADV as:

$$\mathcal{L}_{ADP}(\mathbf{x}, \mathbf{x}_a, \mathbf{y}) = \mathcal{L}_{AT}(\mathbf{x}, \mathbf{x}_a, \mathbf{y}) - ADP_{\alpha,\beta}(\mathbf{x}, \mathbf{y}) - ADP_{\alpha,\beta}(\mathbf{x}_a, \mathbf{y})$$

### Model architecture and training setting

We use both standard CNN architecture and ResNet architecture in our experiment. For ResNet architecture, we use the same architecture and training setting as in (Pang, Xu, et al., 2019). More specifically, we use ResNet-20 and Adam optimizer, with initialized learning rate 0.001 and reduce it by a factor 0.1 at epoch 80, 120, and 160. Table 8 summarizes the standard CNN architecture for each ensemble member in our experiments. The architectures for the MNIST and CIFAR10 datasets are identical with those in (N. Carlini and D. Wagner, 2017). We use Adam optimization with learning rate 0.001 for all datasets. Conv(k) represents for the Convolutional layer with k output filters and ReLU activation. Kernel size 3 and stride 1 for every convolution layer. FC(k) represents for the Fully Connected layers with k output filters without ReLU activation. Dropout rate

Table 8: Model architectures for experimental section

MNIST	CIFAR10	CIFAR100
2 x Conv(32)	2 x Conv(64)	3 x Conv(64)
MaxPool	MaxPool	MaxPool
2 x Conv(64)	2 x Conv(128)	3 x Conv(128)
MaxPool	MaxPool	MaxPool
FC(200), ReLU	FC(256), ReLU	FC(256), ReLU
Dropout(0.5)	Dropout(0.5)	Dropout(0.5)
FC(200), ReLU	FC(256), ReLU	2 x (FC(256), ReLU)
FC(10)	FC(10)	FC(100)
Softmax	Softmax	Softmax

Table 9: Comparison on the training time on the CIFAR10 dataset using ResNet architecture

Model	N=2	N=3
ADV (N=1)	109s	109s
ADV-EN	205s	319s
ADP	210s	328s
Ours	356s	546s

is 0.5. We train models in 180 epochs for both CIFAR10 and CIFAR100 datasets and in 100 epochs for the MNIST dataset.

**Comparison on the training time.** Our method requires to find the adversarial examples of each member and do cross inference, therefore, it takes a longer training process. We measured the training time (per epoch) on our machine with Nvidia RTX Titan GPU, using ResNet architecture (N=2,3) with batch size 64 on the CIFAR10 dataset and summarize as in Table 9.

### White-box attacks evaluation

In addition to the result in the experimental section, we provide further results on the evaluation of adversarial robustness under white-box attacks. Firstly, we explain in detail the metrics of interest in our experiments. Secondly, we provide an ablation study to show the impact of the transferring flow to the improvement.

### Robustness evaluation metrics

**Static attack and Adaptive attack.** There are two scenarios of attacks on an ensemble model (W. He et al., 2017). The first scenario is *static attack*, in which the attacker is not aware of the ensemble method (i.e., how to do the ensemble for making the final prediction). The other scenario is *adaptive attack*, where the attacker has full access to the ensemble method and adapts attacks accordingly. In our experiments, we make use of the adaptive attack, which is a considerably stronger attack.

**Non-targeted attack and Multiple-targeted attack.** We use both non-targeted attack ( $\mathcal{A}$ ) and multiple-targeted attack ( $mul\mathcal{A}$ ) in our evaluation. The non-targeted attack obtains adversarial examples by maximizing the loss w.r.t its true label, resulting in any non-true label prediction. The

Table 10: Ablation study on the impact of the transferring flow. Note that *mulA* represents for the multiple-targeted attack by adversary  $\mathcal{A}$ .

(a) Evaluation on CIFAR10 dataset. We commonly use  $\epsilon = 8/255, \eta = 2/255$

	ADP <sub>2</sub>	CCE-Base <sub>2</sub>	CCE-RM <sub>2</sub>	ADP <sub>3</sub>	CCE-Base <sub>3</sub>	CCE-RM <sub>3</sub>
Non-att (Nat. acc.)	75.9	75.8	<b>76.0</b>	76.6	76.4	75.7
PGD $k = 100$	42.2	43.4	<b>44.7</b>	43.9	44.5	<b>46.8</b>
BIM $k = 100$	42.2	43.4	<b>44.9</b>	43.8	44.5	<b>46.8</b>
MIM $k = 100$	42.4	44.1	<b>45.4</b>	44.2	45.0	<b>47.2</b>
mul-PGD $k = 20$	27.8	31.1	<b>31.9</b>	32.4	32.4	<b>36.9</b>
mul-BIM $k = 20$	27.2	30.8	<b>31.6</b>	29.8	32.2	<b>34.1</b>
mul-MIM $k = 20$	28.3	31.5	<b>32.3</b>	30.7	32.9	<b>34.6</b>
SPSA	41.5	44.3	<b>45.2</b>	46.1	47.2	<b>47.5</b>
Auto-Attack	24.4	29.2	<b>29.9</b>	28.1	31.5	<b>31.9</b>

(b) Evaluation on CIFAR100 dataset. We commonly use  $\epsilon = 0.01, \eta = 0.001$

	ADP <sub>2</sub>	CCE-Base <sub>2</sub>	CCE-RM <sub>2</sub>	ADP <sub>3</sub>	CCE-Base <sub>3</sub>	CCE-RM <sub>3</sub>
Non-att (Nat. acc.)	48.0	51.1	<b>53.4</b>	52.6	54.2	<b>54.4</b>
PGD $k = 100$	30.9	33.6	<b>35.3</b>	36.2	37.0	<b>39.5</b>
BIM $k = 100$	31.0	33.7	<b>35.2</b>	36.2	37.1	<b>39.4</b>
MIM $k = 100$	30.8	33.5	<b>35.3</b>	36.1	37.2	<b>39.6</b>
mul-PGD $k = 20$	20.1	23.0	<b>24.2</b>	24.8	26.2	<b>28.4</b>
mul-BIM $k = 20$	19.4	22.6	<b>23.7</b>	24.5	25.9	<b>28.1</b>
mul-MIM $k = 20$	20.3	23.1	<b>24.1</b>	25.1	26.4	<b>28.6</b>
SPSA	24.1	<b>32.1</b>	31.8	32.5	<b>35.1</b>	35.0
Auto-Attack	14.8	<b>22.0</b>	21.9	23.0	<b>26.1</b>	25.9

multiple-targeted attack is undertaken by performing simultaneously targeted attacks for all possible data labels (10 for CIFAR10 and 100 for CIFAR100) and being counted if any individual targeted-attack is successful. While the non-targeted attack considers only one direction of the gradient, the multiple-targeted attack takes many directions into account, therefore, being considered as a much stronger attack.

### Ablation study

We provide an ablation study to compare CCE-RM with CCE-Base (which disables promoting and demoting operations by setting  $\lambda_{pm} = \lambda_{dm} = 0$ ). Firstly, the comparison in Table 10 shows that even CCE-Base variant can beat ADP method on both CIFAR10 and CIFAR100 datasets. This surpassness can be explained from the fact our proposed method encourages the diversity of its committee members. More specifically, each member is reinforced with two data sources: clean data  $\{\mathbf{x}\}$  and adversarial examples  $\{\mathbf{x}_a^n\}$ , which becomes more diverge due to the gradually more divergence of the committee models and the random initialization of PGD at the step 0. From this point of view, our method can be linked to the bagging technique in traditional ensemble learning, which is a well-known method to produce the diversity in the ensemble. Secondly, CCE-RM shows a huge improvement over CCE-Base in both CIFAR10 and CIFAR100 datasets. This result demonstrates the impact of the transferring flow, which offers better collaboration among members.

In addition, we study the impact of each PO and DO to the final performance by evaluating them separately. Table 11 shows the comparison when disabling one of these operations while varying the other. It can be observed that: (i) the ensemble tends to be detection mode (i.e., increasing natural performance and adversarial detectability while sacrificing its robustness) when increasing DO’s strength ( $\lambda_{dm} \geq 2$ ),

Table 11: Ablation study on the impact of each operation PO/DO. We commonly use  $\epsilon = 8/255, \eta = 2/255$ . Note that *mulA* represents for the multiple-targeted attack by adversary  $\mathcal{A}$ .

(a) Using DO only by disabling cPO ( $\lambda_{pm} = 0$ )

	$\lambda_{dm} = 0$	$\lambda_{dm} = 1$	$\lambda_{dm} = 2$	$\lambda_{dm} = 5$
Non-att (Nat. acc.)	75.8	76.6	83.2	86.0
PGD $k = 100$	43.4	43.3	23.9	26.1
BIM $k = 100$	43.4	43.2	24.0	26.2
MIM $k = 100$	44.1	43.6	31.1	21.7
mul-PGD $k = 20$	31.1	29.9	14.9	20.1
mul-BIM $k = 20$	30.8	29.8	13.1	19.8
mul-MIM $k = 20$	31.5	30.3	28.6	21.7
SPSA	44.3	44.4	30.4	5.3
Auto-Attack	29.2	29.8	1.6	0.2

(b) Using PO only by disabling DO ( $\lambda_{dm} = 0$ )

	$\lambda_{pm} = 0$	$\lambda_{pm} = 1$	$\lambda_{pm} = 2$	$\lambda_{pm} = 5$
Non-att (Nat. acc.)	75.8	76.4	76.2	77.1
PGD $k = 100$	43.4	42.7	42.7	41.3
BIM $k = 100$	43.4	42.8	42.7	41.5
MIM $k = 100$	44.1	43.0	43.2	41.9
mul-PGD $k = 20$	31.1	30.4	30.0	29.7
mul-BIM $k = 20$	30.8	30.3	29.9	29.6
mul-MIM $k = 20$	31.5	30.8	30.4	30.1
SPSA	44.3	44.3	45.5	46.2
Auto-Attack	29.2	29.7	28.8	30.0

(ii) the ensemble tends to reduce its robustness slightly when increasing PO’s strength, (iii) neither PO nor DO can improve the robustness alone, which shows the important of the transferring flow. These observations are inline with the properties of PO and DO which have been mentioned in the main paper. The parameter  $\lambda_{pm}(\lambda_{dm})$  controls the level of the agreement (disagreement) of models  $\{f^i, i \in [1, N]\}$  and model  $f^j, j \neq i$  on the same adversarial example  $x_a^j$ . Therefore the observation (i) can be explained by the fact that by disabling cPO ( $\lambda_{pm} = 0$ ) and strengthening DO, our method encourages the disagreement among members on the same data example, therefore, increases the negative correlation among them. In contrast, by disabling DO and increasing cPO’s strength, our method increases the agreement among members, therefore, increases the positive correlation. The increasing of the positive correlation among members reduces the diversity of adversarial space, therefore, explains the observation (ii).

### Black-box attacks evaluation

We investigate the transferability of adversarial examples among models and evaluate the robustness under black-box attacks. The experiment is conducted on the CIFAR10 and CIFAR100 datasets, with ensemble of two members. We use PGD to challenge each ensemble model to generate adversarial examples then transfer these adversarial examples to attack other models. The PGD configuration for the CIFAR10 dataset is  $k = 20, \eta = 2/255, \epsilon \in \{8/255, 12/255\}$ , while that for the CIFAR100 dataset is  $k = 20, \eta = 0.001, \epsilon \in \{0.01, 0.02\}$ . The result is shown in Figure ??.

Table 12: Blackbox attack evaluation on CIFAR10 dataset

(a) PGD attack with  $k = 20, \epsilon = 8/255, \eta = 2/255$ 

	NAT	ADV-EN	ADP	CCE-RM
NAT	9.2	76.2	75.6	74.5
ADV-EN	59.5	40.7	58.5	58.4
ADP	58.4	61.8	42.9	59.9
CCE-RM	57.3	58.9	57.4	45.5

(b) PGD attack with  $k = 20, \epsilon = 12/255, \eta = 2/255$ 

	NAT	ADV-EN	ADP	CCE-RM
NAT	8.0	75.5	75.1	74.0
ADV-EN	40.1	23.6	44.5	45.2
ADP	38.4	48.5	24.9	47.1
CCE-RM	35.9	42.9	41.3	27.8

Table 13: Blackbox attack evaluation on CIFAR100 dataset

(a) PGD attack with  $k = 20, \epsilon = 0.01, \eta = 0.001$ 

	NAT	ADV-EN	ADP	CCE-RM
NAT	14.7	43.6	49.3	52.9
ADV-EN	42.9	31.1	48.1	51.6
ADP	41.8	41.6	32.8	50.9
CCE-RM	39.4	40.2	45.8	36.1

(b) PGD attack with  $k = 20, \epsilon = 0.02, \eta = 0.001$ 

	NAT	ADV-EN	ADP	CCE-RM
NAT	13.0	43.6	49.2	52.9
ADV-EN	39.9	24.3	46.9	50.4
ADP	38.3	40.6	25.2	49.4
CCE-RM	34.5	38.2	43.0	27.5

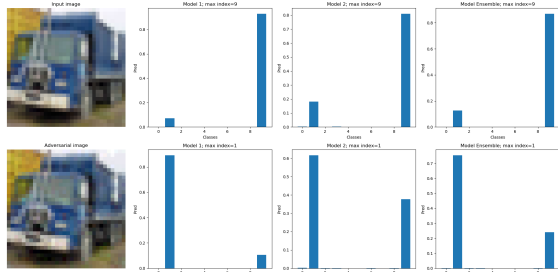
The element  $a^{(i,j)}$  in each sub-table represents the robust accuracy when adversarial examples from model  $i$  attack model  $j$ . *NAT* represents for the natural model which does not engage with any defense method. It is worth noting that, the diagonal in each sub-table represents robust accuracies against the white-box attacks, which has been discussed in the section above.

Firstly, the first row in each sub-table shows the robust accuracy against adversarial examples which are transferred from the natural model (*NAT*). This result shows that our method outperforms baseline methods on the CIFAR100 dataset, but to be weaker than other on the CIFAR10 dataset. Secondly, each column in each sub-table compares the attack strength of different models on the same defense model. The comparison on these columns shows that adversarial examples which are crafted from our CCE-RM attack better than those crafted from other methods (i.e., by giving lower robust accuracy). This result indicates that our method generates stronger adversarial examples than other methods.

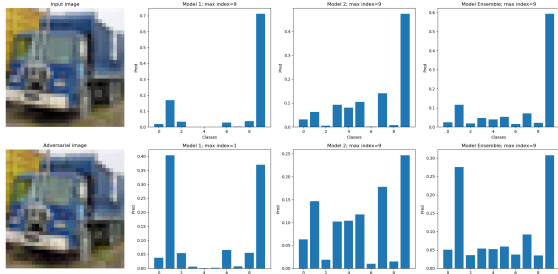
### Loss surface visualization

In addition to the quantitative evaluation on the adversarial robustness, we would like to provide two additional visualizations which further demonstrate our improvement. The visualizations are conducted on the same image from CI-

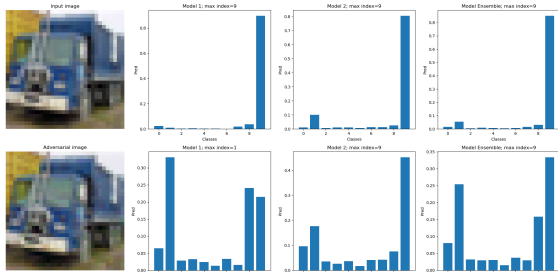
FAR10 dataset with the ensemble of two models. First, we visualize the prediction probability of each ensemble member and the entire ensemble with the same two types of input which are a benign example and adversarial example of the benign one. The visualization as Figure 5 shows that our method can produce a high confident prediction unlike ADP which has a less confident prediction because of its diversity promoting method. Secondly, we visualize the loss surface around the adversarial example  $\mathbf{x}_a$  w.r.t three different of model:  $f^1, f^2$  and  $f^{en}$ . We generate a grid of neighborhood images  $\{\mathbf{x}_a + i * u + j * v\}$  where  $u = \nabla_{\mathbf{x}} \mathcal{C}(f(\mathbf{x}_a), \mathbf{y})$  is the gradient of the prediction loss w.r.t the input and  $v$  is the random perpendicular vector to  $u$ . In each sub-figure, the left image is the adversarial example of interest while the middle and the right image depict the loss surface and the predicted labels corresponding with the neighbor grid. Our method can produce correct labels in entire the neighborhood region, unlike other methods that still have an incorrect prediction region. Therefore, our method can produce a smoother surface around the adversarial example which further explains the better robustness in our method.



(a) ADV-EN.

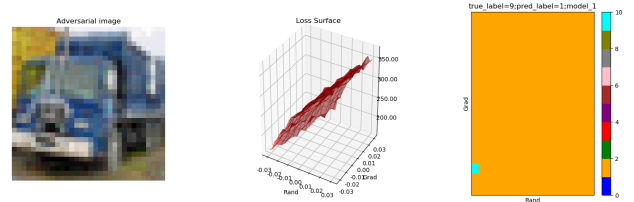


(b) ADP.

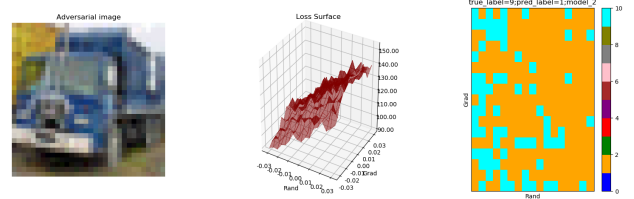


(c) CCE-RM.

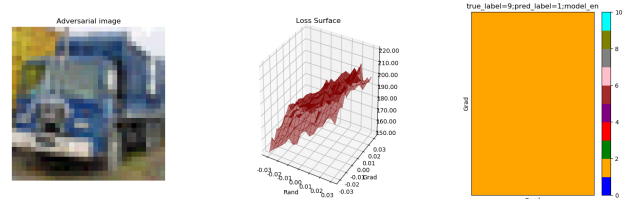
Figure 5: Prediction example. Top/bottom images are benign/adversarial images. Next columns are outputs from  $f^1, f^2, f^{en}$ .



(a) Prediction surface of model  $f^1$ .

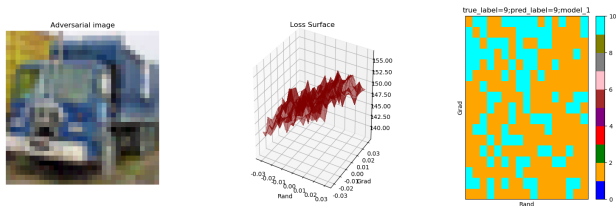


(b) Prediction surface of model  $f^2$ .

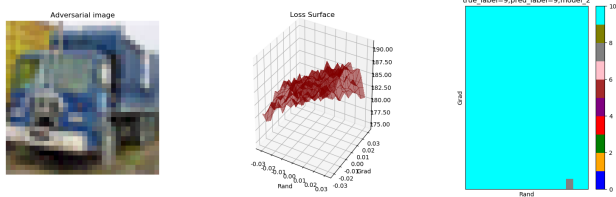


(c) Prediction surface of model  $f^{en}$ .

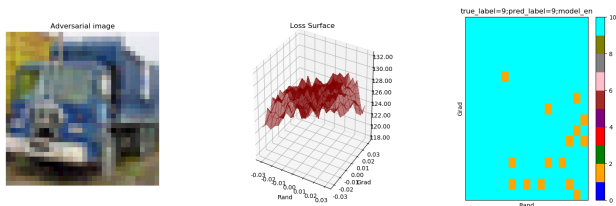
Figure 6: Loss surface around adversarial example of ADV-EN method. Left: Adversarial input. Middle: Loss surface. Right: Predicted labels.



(a) Prediction surface of model  $f^1$ .

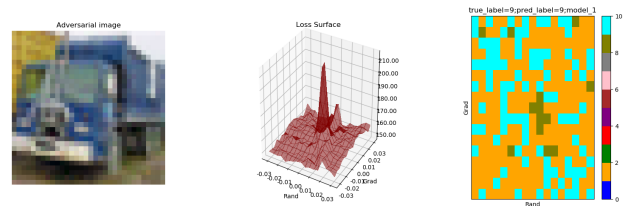


(b) Prediction surface of model  $f^2$ .

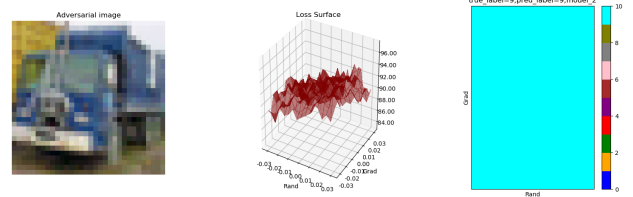


(c) Prediction surface of model  $f^{en}$ .

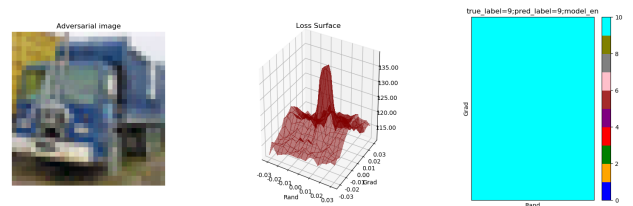
Figure 7: Loss surface around adversarial example of ADP method. Left: Adversarial input. Middle: Loss surface. Right: Predicted labels.



(a) Prediction surface of model  $f^1$ .



(b) Prediction surface of model  $f^2$ .



(c) Prediction surface of model  $f^{en}$ .

Figure 8: Loss surface around adversarial example of CCE-RM method. Left: Adversarial input. Middle: Loss surface. Right: Predicted labels.